IC/94/166
INTERNAL REPORT
(Limited Distribution)

International Atomic Energy Agency
and
United Nations Educational Scientific and Cultural Organization
INTERNATIONAL CENTRE FOR THEORETICAL PHYSICS

MODELLING THE DAY TO DAY WIND VARIABILITY OFFSHORE CENTRAL CHILE AT ABOUT 30 DEG. SOUTH

Jose Rutllant[1]
International Centre for Theoretical Physics, Trieste, Italy.

ABSTRACT

Cycles of strengthening and relaxation of the winds offshore 30 degrees S at central Chile, are related to the propagation of coastal-lows, a year- round phenomenon occurring with periodicities of about one in five days.

Simple physical modelling of the day to day variability of the alongshore wind component at a coastal strip extending offshore up to the Rossby deformation radius of these wave perturbations, is presented in terms of the relevant horizontal pressure gradie nts and the ageostrophic components arising from the coastal-low propagation.

The results of 5-day composites of 8 wind-events each, at the winter and summer halves of the annual cycle, respectively; lead to a good agreement between the observed phase-lag of the winds with respect to the pressure forcing field, stressing the importance of the ageostrophic wind components at the extremes of the pressure wave perturbation associated with the passage of coastal-lows over the Point Lengua de Vaca (30 15 S) area.

A possible contribution to the upwelling-favorable wind enhancement at the time of the pressure rise and subsequent fall, ahead of the coastal-low, is postulated through an upwelling-front low-level jet, that would be carried onshore and closer to the surface by the combination of the enhanced coastal upwelling, the coastal depression of the subsidence inversion base and the coastal ageostrophic wind components during the passage of the leading edge of the coastal lows.

MIRAMARE – TRIESTE

July 1994

[1]Permanent Address: Department of Geophysics, Universidad de Chile, Casilla 2777, Santiago, Chile.

1 Background

The wind regime at Point Lengua de Vaca, located at 30 15 S on the west coast of South America, nearby one of the foremost upwelling-active areas of the subtropical chilean coast, presents a typical diurnal cycle with minimum speeds at about 9 am and a well-defined maximum in the late afternoon, when winds blow from the SW with 30-min-average speeds exceeding sometimes 15 ms-1 (Rutllant, 1994a).

Progressing offshore, the daily-cycle signal of the wind decreases in amplitude, remaining only the high wind speeds and direction that characterize the diurnal phase at the coast, as discussed for the CODE area in California by Beardsley et al., (1987).

In addition to the daily-cycle signal, irregular alternances of strong and weak alongshore winds with recurrence periods of about one every 5 days, have been documented for Point Lengua de Vaca in Rutllant (1993, 1994a). At this site, those wind transitions are coherent in time with changes in the cloud cover and surface pressure. In fact, clear skies occur during the strong alongshore winds, at the time when the pressure reaches a maximum and decreases sharply thereafter, while stratocumuli overcasts coincide with the wind relaxations and with the pressure rising after reaching a minim um value associated with the passage of a "coastal-low" (Rutllant, op. cit.).

In terms of wind-driven coastal upwelling, the offshore area affected by those wind events extends roughly up to 100 km offshore, as revealed by satellite imagery (Uribe and Neshiva, 1983).

The coastal-low related cycles have their origin in weak mid-latitude frontal disturbances that become blocked against the topography to the north of the study area (Rutllant, 1994b). The blocking results in internal gravity waves at the subsidence inversion interface, propagating from north to south while trapped along the coast by the Coriolis effect. The offshore influence of these waves should theoretically extend up to R, the $e-1$ folding distance of the amplitude of the wave away from the coastal escarpment, known as the Rossby radius of deformation (Gill, 1982). Estimations for this area yield R values around 180 km (Rutllant, 1994b).

Due to their origin, coastal lows are observed as a year-round phenomenon, with a periodicity closely tied to the typical synoptic-scale variability of the mid-latitude western South America.

One of the most important features of the propagation of these waves along the coast, is the oscillation of the base of the subsidence inversion, that separates the cool and well mixed marine atmospheric layer below from the warm, dry and stable subsiding air above it. These oscillations are responsible for the cloud-cover and mixed-layer changes associated with the coastal lows.

Besides the effect of the leading edge of the coastal lows in bringing the inversion layer down (Reason and Jury, 1990; Rutllant, 1994b), the position of that interface depends on the height-integrated divergence of the flow within the marine layer, associated to both the southeastern subtropical anticyclone and other regional-scale phenomena. It also depends on the turbulent kinetic energy generated by shear and buoyancy within the marine layer; the latter being mainly produced through radiative cooling of the could deck top frequently present in these areas (Fuenzalida, 1985).

Radiosonde measurements at some stations along the west coasts of the Americas, have shown that the base of the inversion layer is closer to the ground in the afternoon (Neiburger et al., 1961; Rutllant and Ulriksen, 1979). This would be mainly due to the

land-ocean temperature contrast brough about by the insolation cycle overland and by the resulting atmospherere and ocean circulations that feedback upon this land-sea thermal forcing.

The purpose of the present work is to set the framework for a simple modelling of the day to day alongshore wind variability in a coastal strip exposed to wind-driven upwelling and to the offshore effects of coastally- trapped atmospheric internal gravity waves (coastal-lows). By means of basic physical relationships, the wind variability associated with a composite strengthening-relaxation cycle of 5 days, will be discussed for the extreme seasons.

As a result of the inherent simplifications and of other processes not accounted for, together with the use of extrapolated data from coastal observations, empirical adjustment factors have to be included in the model. The approach followed here is basically geostrophic, implying that consideration of the most relevant processes leading to horizontal pressure gradients, including their time and space changes, during the life-cycle of the fast-speed propagating coastal lows have to be included.

Section 2 considers the meteorological factors that shape the marine layer of the subtropical southeastern Pacific, including their most relevant baroclinic zones in a west to east cross-section.

In Section 3, low-level-jet (LLJ) structures and mechanisms along the west coast of North America will be analized. A slightly different version for the South American case will be proposed.

The parameterizations of the large-scale horizontal pressure gradient and of the ageostrophic contributions to the alongshore flow within the area, will be dealt with in Sections 4 and 5, respectively.

The formulation of the model describing the behaviour of the coastal upwelling system in response to the forcing pressure-gradient fields and the qualitative comparison with actual 5-day composites of eight wind-events in winter and eight in summer, will follow in Section 6.

A final Section summarizes the results and discusses further work to improve the time and space resolutions ob the observations along the coast and offshore.

2 The Subsidence in the Subtropical SE Pacific

The west to east increase in subsidence and the corresponding descent of the inversion layer are common factors of the eastern sectors of the subtropical anticyclones (Schubert, 1976), in part associated with the cold eastern-boundary ocean currents flowing equatorward along the west coasts of the conti nents.

Direct observations of the sloping inversion base have been documented for the California area. A concise review of the main results is presented in Dorman (1987).

For the chilean coast, only a few scattered airborne measurements have been performed. Two pairs of coastal and 50 km offshore vertical temperature profiles at 9 hours LT, obtained in November 1987 at 29.5 S (Fuenzalida et al., 1990), will be discussed in Section 3.

The slope of the inversion interface can be indirectly inferred from satellite pictures during the afternoon. At this time, the depressed inversion causes the mixing condensation level of the stratocumulus clouds to fall above its base, producing cloud-free conditions.

This frequent offshore clear area follows approximately the coastal shape, suggesting the importance of land-ocean thermal and roughness differences in shaping the subsidence enhancement along the coastline.

Conversely, after a frontal disturbance has progressed northwards along the coast, leaving clear skies or at most open fair-weather cumuli cells, the marine layer is lifted against the orography, producing a coastal band of stratiform cloudiness with almost clear skies further offshore. The resulting thickening of the marine layer against the coastal mountains is supposed to lead to the formation and subsequent southwards propagation of the coastal lows, as explained before.

2.1 Baroclinic zones in a west-east cross section

Mean baroclinic strips in a zonal cross section of the marine layer, including a coastal upwelling area, are depicted in Figure 1. From left to right, there is a first zone across the climatological position of the "upwelling front", defined as the zone where SST's (sea-surface temperatures) present their largest gradient in the zonal direction.

Above the upwelling front, the direction of the thermal wind coincides with the southerly surface alongshore geostrophic wind component. Also, as it will be discussed later, the slope of the subsidence inversion base above it should be enhanced, as the marine layer tends to become thinner on the colder side (onshore). Therefore, opposite tilts of the pressure surfaces within and at the top of the marine layer, produce a geostrophic wind maximum immediately below the base of the inversion layer.

Another important baroclinic zone forms across the coastline due to the average land-sea thermal contrast. In this case the alongshore thermal wind is northerly, leading to a near-surface southerly wind maxima. Here, since the cold-water upwelling along the coa st is basically wind-driven, it reinforces the alongshore winds themselves through an increased land-sea thermal contrast, resulting into a positive feedback mechanism. In addition to that, the air-sea circulation feedback results particularly efficient he re, since at these latitudes the inertial period coincides approximately with the insolation forcing cycle.

A third baroclinic zone above the inland mountain slopes (Lettau 1967; Rutllant 1977, 1990) should not play an important role in the day to day variability associated with coastal lows propagation, since the changes in cloud cover are limited to a narrow coastal strip due to the average sloping topography.

Superimposed on the precedent factors that contribute to shape the average west to east slope of the subsidence inversion base, the oscillations resulting from the day-night insolation cycles and the coastal-low cycles will periodically reinforce or weaken the average circulation features associated with the relevant baroclinic zones.

3 The Low-Level Jets in the Marine Layer

Climatological evidences of the offshore wind maxima at an average distance of 300 km from the coast, based on ship historical records, are given in Bakun and Nelson (1991). However, local airborne measurements documented by Elliott and O'Brien (1977), show a LLJ associated with an enhanced slope of the subsidence inversion base one order of magnitude closer to the coast.

Airborne wind profiles performed during a period of strong upwelling- favorable winds at the California coast (Beardsley et. al, 1987), revealed that the maximum winds occur at about the level of the base of the subsidence inversion a few tens of km offshore, at a point where its general eastward downslope reaches a maximum. The low-level jet (LLJ) structure of the winds would be due, according to these authors, to the baroclinicity associated with the slope of the inversion, where the thermal-wind relationship (warm onshore- cool offshore) would strengthen the equatorward (alongshore) geostrophic wind components within the inversion down to its base. From the jet core down to the surface, the wind profile structure would be explained by the vertical divergence of the shear stresses (Zemba and Friehe, 1987). These authors also suggest that a small thermal-wind component within the marine layer would be due to the west to east decrease in SST.

According to Beardsley et. al (1987), the major effect of the daytime insolation inland would be to bring onshore this LLJ with the corresponding area of maximum inversion-base tilt, producing the observed daytime increase in the windspeed and the descent of the base of the inversion at the coast. The return flow of the sea-breeze system would also contribute to the coastal subsidence enhancement. These authors also point o ut that the wind-relaxations between periods of strong winds, coincide with a lifting or disruption of the inversion layer.

The lack of airborne wind data off central Chile makes it difficult to test the validity of the above mechanisms. However, if we assume that at distances of the order of 10 to 30 km from the coast the general wind direction within and above the inversion does not differ substantially from measurements at the coastal radiosonde stations of Antofagasta (23 S) and Quintero (33 S), we could conclude that easterly wind flow veering to northwesterly aloft is more common than equatorward flow, in agreement with the thermal-wind structure related to the sloping inversion.

A review of other meteorological studies in coastal-upwelling regions presenting jet-like patterns in the vertical wind profiles is included in Zemba and Friehe (1987). In terms of the proposed mechanims to explain the jet, Bunker (1965), Lettau (1967, 1978) and Enfield (1981) refer to the the diurnal baroclinic coastal zone where the land-ocean temperature differences are enhanced due to the positive feedback upon the wind-driven coastal upwelling. Conversely, Zemba and Friehe (1987) themselves, following previous work, support the scheme described above, where thermal wind arg uments apply in the upper sector of the jet, above its high-speed core.

In quantitative terms, the LLJ observations by both Beardsley et al. (1987) and Bunker (1965) coincide in a 10 to 15 ms-1 difference in speed from the sea surface or from above the inversion, to the jet core. Similar windspeed differences from the surface to the jet core have been obtained from coastal pilot-balloon observations during upwelling-favorable wind events at 30 S in central Chile during the austral summer (Rutllant, 1993).

3.1 The upwelling front off 30 S in central Chile.

AVHRR satellite data of the coastal SST structure, obtained during the field surveys carried out at 29.5 S in november 1987 and 1988, revealed an average position of the upwelling front at 45 and 80 km offshore, respectively. Typical cross-front SST gradients were of the order of 1.5 C / 10 km (Rutllant et al., 1994). These upwelling fronts, separating coastal upwelled waters with temperatures around 13 C from oceanic waters of 17 to 18 C, also constitute the boundary between the wind-driven coastal equatorward

flow and a countercurrent offshore, especially strong and close to the coast during the El Nino years, like in 1987. The opposite phase of that El Nino / Southern Oscillation cycle, as attained in 1988, is characterized by weaker countercurrents, normally under the surface.

Therefore, large-scale ocean circulation changes and coastally-traped Kelvin waves propagating alongshelf can significantly affect the result of a given wind event in terms of the ocean thermal response and the offshore extension of the cold upwelling plumes.

During the 1987 field experiment, a few airborne measurements were aimed at the comparison of the 12 UTC (09 LT) vertical temperature profiles at the coast and 50 km offshore (Fuenzalida et al., 1990). Measurements at that time coincided with the peak of a wind event on November 6 and 7, 1987. Vertical temperature profiles, obtained with a Rosemont airborne thermometer and the airplane altimeter, are depicted in Figure 2 for both days. The inversion-base levels were 80 m and 180 m higher in the offshore soundings on the 6th and 7th, respectively. Disregarding any offshore differences in the tilt of the subsidence inversion base arising from the daily cycle at that time and in the coastal-low effect because of the relatively short distance from the coast compared with the Rossby radius, a SST difference of 4 C would produce the observed change in the marine layer depth. In fact, according to Hsu (1988):

$$\text{DELTA } h = 30 + 29.8 \text{ DELTASST} \qquad \begin{matrix}\text{DELTA}h = \Delta h \\ \text{DELTASST} + \Delta\text{SST}\end{matrix}$$

where h is the depth of the marine layer (base of the subsidence inversion) in meters, and DELTASST is the sea-surface temperature (SST) difference in degrees C.

Since in 1987 the upwelling front was at about 45 km offshore, the 4 C difference in SST is compatible with normally observed SST differences between coastal and oceanic waters during upwelling events.

3.2 The upwelling-front LLJ

By a simple application of the thermal-wind equation, it can be shown that the characteristic gradient across the upwelling front, estimated in about 1.5 C /10 km (Section 3.1), leads to the top to bottom geostrophic wind difference within the marine layer in close agreement with those found elsewhere, including measurements at Point Lengua de Vaca (30.15 S), just north of the main upwelling focus (Rutllant, 1993).

If V_{gh} is the geostrophic wind at the top of the marine layer and V_{go} is the ocean-surface one; < SST > and DELTASST are the average temperatures within the marine layer and the SST difference at both sides of the upwelling front, respectively, we can write

$$V_{gh} - V_{go} = R_d f^{-1}(ln1/(1 - h_g/R_d < \text{SST} >))\text{DELTASST}/2\text{DELTA}x$$

where h is the top of the marine layer (base of the inversion), R_d is the gas constant for dry air, f is the Coriolis parameter, g is gravity and DELTASST /DELTAx is the SST gradient across the front. The factor 2 in the denominator accounts for the quasi-linear decrease of the temperature difference, from DELTASST at the surface to zero close to the inversion base (Figure 1). A geostrophic wind difference of 15 ms-1 results if the inversion base is set at 400 m and < SST >= 288 K. Reducing the marine layer depth to 200 m, the difference between the top and bottom alongshore geostrophic winds would be of 8.3 m s-1.

Therefore, given the observed wind structure within and above the coastal inversion layer in central Chile, and the results obtained here, a LLJ above the upwelling front is postulated. Evidently, the sharp decrease in speed above the jet maximum speed is produced by the enhanced tilt of the inversion base.

Now, in the sunny afternoons characterizing the strongest upwelling- favorable winds ahead of the passage of the coastal lows, the jet-like structure of the coastal winds could be a combination of the land-sea thermal-contrast LLJ an d a component of the upwelling-front jet.

The contribution of the upwelling-front jet would occur in connection with the sharp downward displacement of the inversion base produced by the leading edge of the coastal low and by the diurnal subsidence and upwelling enhancement mechanisms along the coastline. In these circumstances, the LLJ would become elongated onshore and progressively closer to the surface in the onshore direction. Now, the ageostrophic wind components that develop during this stage have on shore components that would help bringing the high-speed wind area towards the coast, contributing to the observed jet-like structure. To test this hypothesis, detailed numerical modelling of both jets should be performed.

However, an onshore drift of a high-speed wind area off Point Lengua de Vaca can be observed in some mornings, coinciding with strong upwelling- favorable winds in the afternoon, as evidenced by fast northward moving stratus patches detached from the strato-cumulus layer farther offshore and by white caps, contrasting with the near-calm surface conditions at the sea-shore. Whether this effect is caused by the mechanism suggested by Beardsley et al. (1987) or by the ageostrophic wind components does not seem easy to dilucidate, since the sea-breeze is also part of the total ageostrophic wind flow.

The progressive offshore extension of the upwelling front through the wind event will cause the coastal winds to weaken somewhat as the center of the low approaches the area.

4 Large-Scale Horizontal Pressure Gradient

In order to represent the daily average large-scale pressure gradient contributing to the geostrophic component of the alongshore winds in the study area, sea-level pressures (SLP's) and winds measured at San Felix island (26 20 S, 79 58 W), about 930 km (d) to the NW of Point Lengua de Vaca, are used to estimate a SLP value at 180 km (R) from the coast, supposedly at the western boundary of the coastal-low influence.

Values of SLP have been taken at 21 UTC, corresponding approximately to the time of the peak of the diurnal phase of the coastal winds and to the daytime minima of the SLP's (Rutllant, 1994a), when diurnal and semidiurnal atmospheric-tide effects are not removed.

The SLP value to be considered at the western boundary of the study area, is calculated as

$$\mathrm{SLP}(R) = \mathrm{SLP}_{sf} - \partial \mathrm{SLP}_{sf}/\partial x \times 750\mathrm{km}$$

where SLP(R) corresponds to the SLP at $x = -R$, with a zonal coordinate $x = 0$ at the coastline. This value is calculated substracting from the SLP_{sf} the slope of the pressure field in the x direction, as given by the daily mean alongshore winds at San Felix (V_{sf}),

which are assumed to be in geostrophic equilibrium and to represent a wide area around the station.

Now, the zonal SLP gradient across the study area can be written as SLP(R) - SLP_{lv}, where SLP_{lv} is the 21 UTC SLP value at Point Lengua de Vaca. Therefore, an average surface geostrophic alongshore wind V_g in the study area would be

$$V_g = (\rho[f]R)^{-1}(\mathrm{SLP}_{sf} - \rho[f](d - R)V_{sf} - \mathrm{SLP}_{lv})$$

where both, the air density ρ and the absolute value of the Coriolis parameter [f] are considered constants.

If the SLP's are expressed in hPa and the windspeeds in m $s-1$, with $f = 6.8 \times 10-5s-1$ (28 S) and $\rho = 1.3$ kg m-3, the resulting expression for the geostrophic component at the coastal strip is

$$V_g = 6.3(\mathrm{SLP}_{sf} - \mathrm{SLP}_{lv}) - 4.2V_{sf}$$

The surface stress of the winds can be calculated following the geostrophic drag coefficient (C_g) approach (see, for instance, Garratt, 1992) where C_g is a function of the surface Rossby number R_o

$$C_g = ((u * o)/V_g)^2 = f(R_o), \text{ with } R_o = V_g/[f]zo$$

Here, the surface roughness zo, though relatively small, will depend on the waves at the ocean surface (Hsu, 1988).

5 The Ageostrophic Wind Components

Assuming that friction is being accounted for at the surface through the geostrophic drag coefficient, the acceleration of an inviscid fluid element for a rotating flow in the f-plane, can be represented by the equation (see for instance, Haltiner and Martin, (1957)):

$$d\vec{V}/dt = f(\vec{V} - \vec{V}_g) \times \vec{k} = \partial V/\partial t + V\partial\vec{V}/\partial s + w\partial\vec{V}/\partial z$$

where $\vec{V}$ is the wind vector with speed V, s is the horizontal trajectory of the fluid element, w is the vertical component of the wind vector, and $\vec{k}$ represents a unit vector pointing vertically upwards in the z direction.

If in the partial derivatives of the right hand side of the preceding equation $\vec{V}$ is approximated by $\vec{V}_g$, the ageostrophic wind component ($\vec{V}_{ag} = \vec{V} - \vec{V}_g$) can be written as:

$$\vec{V}_{ag} = 1/f\vec{k}x\partial\vec{V}_g/\partial t + \vec{V}/f\vec{k}x\partial\vec{V}_g/\partial s + w/f\vec{k}x\partial V_g/\partial_z$$

$$\vec{V}_{ag} = \vec{V}_{agis} + \vec{V}_{agad} + \vec{V}_{agw}$$

where the first term represents the contribution to the ageostrophic wind component due to the local change of the horizontal pressure gradient, (V_{agis} = isallobaric wind component), the second is the corresponding contribution due to downwind changes in t hat gradient (V_{agad} = horizontal advective wind component) and the third represents the equivalent vertical advective component (V_{agw}).

5.1 The isallobaric component.

The isallobaric contribution to the ageostrophic wind can be written as

$$(\vec{V} - \vec{V}_g)_{is} = -\rho^{-1} f^{-2} \nabla(\partial p/\partial t)$$

where ∇ is the horizontal gradient operator.

This wind component results perpendicular to the lines of constant pressure tendency (isallobars). When added to the geostrophic wind, the resultant flow will be at at an angle with the isobars toward lower pressures.

Along the central coast of Chile, the bulging of the isobars due to the propagating coastal-lows through the eastern boundary of the subtropical anticyclone, results in south-easterly geos trophic winds ahead of the low, so that the V_{agis} component will result in an increase in the alongshore flow and a direction change to the S and SW.

The alongshore contribution of this vector (y direction, positive northward) will be

$$V_{agis} = -\rho^{-1} f^{-2} \partial(\partial p/\partial y)\partial t$$

If we assume a coastal-low as an internal gravity wave propagating at a uniform phase-speed from north to south along the marine-layer upper interface, without amplitude changes in the y direction (frozen low), at constant phase-speed c, and with an exponential decrease of the amplitude in the offshore direction with a scale length R, we can write

$$\partial p/\partial y = 1/c(\partial p/\partial t)$$

where the partial derivatives are both negatives at the leading sector of the coastal low and positive at its trailing edge. Now, since ahead of the low $\partial(\partial p/\partial t)\partial y$ is negative (Figure 3), the V_{agis} will be positive there. That means that c has to be considered positive, although the propagation is from north to south (negative y direction).

Now, replacing the y partial derivative by its time equivalent, we get

$$V_{agis} = -\rho^{-1} f^{-2} c^{-1} \partial^2 p/\partial t^2$$

implying that the maximum contribution to the alongshore winds should occur when the curvature of local rate of change of the pressure is at its maximum negative value.

Taking $c = 12ms - 1$, $f = -0.68 \times 10 - 5s - 1$ (28 S) and the density ρ equal to 1.3 kg m-3; and representing the curvature of the SLPlv at day i as a finite difference scheme, we finally get

$$V_{agis} = -18.6(SLP_{lv}(i+1) - 2SLP_{lv}(i) + SLP_{lv}(i-1))$$

with SLP values in hPa and V_{agis} in m s-1.

In the case of a purely sinusoidal pressure wave, the maximum of V_{agis} would coincide with the moment of the maximum pressure and vice-versa.

5.2 The advective components.

As described in the ageostrophic wind equation, the second and third terms correspond to the horizontal and vertical advective components, respectively. The horizontal one corresponds with the downwind variation of the geostrophic wind. Again, the bulging

of the isobars at the leading sector of the low produces a confluence of the isobars, the opposite being true at the trailing sector.

Considering for simplicity a trajectory s along the y direction only and taking the contribution of this ageostrophic component to the alongshore winds, we have

$$V_{agad} = -V\rho^{-1} f^{-2} \partial(\partial p/\partial y)/\partial y$$

where V_{agad} is the horizontal ageostrophic advective wind component in the alongshore direction and V is the total windspeed. If the partial derivatives with respect to y are replaced by $1/c$ times the partial time derivative, as previouly discussed in the case of the isallobaric component, we can write

$$V_{agad} = -V\rho^{-1} f^{-2} c^{-2} \partial^2 p//\partial t^2$$

which is of the same sign and magnitude of V_{agis} ahead of the low, since c and V are comparable there. The contribution of this term at the trailing edge of the low would not be important since the V values are low. Note that this wind component contains t he total windspeed V, that is intended to be predicted by the model as the system response to the pressure field forcing.

In the ageostrophic advective vertical-wind component, the vertical speed w is assumed to be part of the forcing. In fact, if the mass continuity equation is integrated in the vertical across the marine layer, we have

$$\partial h/\partial t + H(\partial u/\partial x + \partial v/\partial y) = -w_s$$

where the first term considers the displacement of the interface as the top value of w (top boundary condition); w being zero at the surface as the bottom boundary condition. The second term is the average, undisturbed height of the marine layer (II) times the average horizontal wind divergence over the marine layer depth. The term - ws in the right hand side represents entrainment into the marine layer, as produced by the warm, offshore downslope flow that characterizes the leading sector of the propa gating coastal lows in central Chile at the inversion level (Reason and Jury, 1990).

Therefore, if $\partial h/\partial t$ is prescribed as one of the components of the forcing function, for instance derived from average radiosonde observations, it would include both the - w_s, as the real forcing of the oscillations of the base of the subsidence inversion, and the height-integrated horizontal divergence as well.

Then, the expression for the vertical advective component of the ageostrophic wind can be written as

$$\vec{V}_{agw} = \partial h/\partial t f^{-1} \vec{k} \times \partial \vec{V}_g/\partial z$$

This term will only be important in the marine layer above the upwelling front. There, both V_g and $\partial V_g/\partial z$ are directed northward, so we can write

$$U_{agw} = -\partial h/\partial t f^{-1} \partial V_g/\partial z$$

and, since f is negative and $\partial V_g/\partial z$ is positive, a negative $\partial h/\partial t$ at the leading sector of the coastal low will produce an ageostrophic component to the left of the geostrophic wind ($U_{agw} < 0$) and viceversa. Therefore, this vertical advective component at the upwelling front, together with the other ageostrophic components that are stronger near the coast, will enhance the marine layer divergence (convergence) ahead (behind) of the low.

6 The Model Formulation

The result of the parameterization of the large-scale surface pressure gradient V_g and of the isallobaric and advective ageostrophic components associated with the coastal-low propagation, contributing to the alongshore winds in the coastal strip extending offshore up to the Rossby radius, for day (i), can be written as

$$V(i) = \frac{V_g(i) - 18.6(SLP_{lv}(i+1) - 2SLP_{lv}(i) + SLP_{lv}(i-1))}{1 + 1/12(SLP_{lv}(i+1) - 2SLP_{lv}(i) + SLP_{lv}(i-1))}$$

where $V_g(i) = 6.3(SLP_{sf}(i) - SLP_{lv}(i)) - 4.2V_{sf}(i)$.

In order to perform a proper calibration keeping the physical meaning of these relationships, it is necessary to understand the way in which the relevant forcing-variables behave during a typical 5-day cycle associated with coastal-low occurrences at Point Lengua de Vaca.

Two continuous time-series of the surface pseudo-stress (SES) of the winds (Rutllant, 1994a) and SLP at Lengua de Vaca, together with SLP and winds at San Felix island, have been used here. They correspond to periods with simultaneous values of all these variables. One period goes from April 25, 1991 until April 18, 1992, and the other from September 26, 1992 until January 31, 1993.

Within these periods, thirty strong wind events were detected, 9 of them between April and September (winter half of the year), and the rest in the remaining summer half. Eight out of the nine winter events have been selected for the composite analysis, si nce one of them corresponded to a large scale event without an associated coastal-low. To avoid any bias arising from the number of events to be considered in the composite analysis, eight out of the 21 summer occurences have been also selected.

As pointed out before, sea-level pressure data corresponds to values at 21 UTC (17 LT), while the wind data for San Felix are daily-averaged alongshore wind components, calculated out of 8 daily synoptic observations. The daily values of the surface pseudo -stress of the wind (SES) are supposed to be representative of a good portion of the study area, since only the diurnal cycle of the of the wind regime has been considered (Rutllant, 1994a).

All the episodes have been centered on the day 0, when the SLP_{lv}'s reach their minimum value within the 5-day period. They correspond to the following dates

WINTER EVENTS	SUMMER EVENTS
91 05 04	91 10 18
91 06 07	91 10 23
91 07 11	91 10 29
91 08 01	92 01 09
91 08 18	92 10 12
91 09 07	92 11 21
91 09 22	92 11 29
92 04 06	92 12 20

The 5-day composite analysis was performed after removing the average values of all the variables, as listed in Table 1.

WINTER EVENTS	SUMMER EVENTS	
Variable	Average	Average	Units
SLP_{sf}	1020.1	1018.0	hPa
SLP_{lv}	1011.6	1009.0	hPa
SES	33	38	m^2s^{-2}
V_{sf}	4.2	4.2	ms^{-1}

Table 1

Figures 4 and 5 represent the composites for the winter and summer events, respectively. On the overall, they do not differ significantly, except for perhaps a slighly larger period in summer.

In spite of the poor time resolution, several basic features arise from the analysis of the Figures;

a) the high pressures on days -2 and -1 are accompanied by strong winds, while the pressure rises corresponding to days 1 and 2 have low winds.

b) the smooth synoptic-type change of the SLP_{sf} contrast with the high- frequency drop and immediate rise of the SLP_{lv}, in connection with the passage of the coastal low.

c) winds at San Felix are in phase with the pressure changes there, so they do not modify the phase of the large scale forcing given by the SLP_{sf}-SLP_{lv} difference. Conversely, a one-day lag is apparent in the winds with respect to the pressure at Point Lengua de Vaca.

d) the large-scale pressure-gradient forcing represented by SLP_{sf} - SLP_{lv} is at its peak during day 0, when the winds at Lengua de Vaca have already decreased substantially.

In summary, during days -2 and -1 the strength of the coastal winds, as represented by the SES, is enhanced due to a combination of the large-scale forcing, represented by the pressure rise following a frontal disturbance, and the ageostrophic wind compone nts associated to the leading edge of the coastal low. During days 0 and 1, both forcing agents bring the winds to a minimum, in particular during day 1 when the negative contribution of the ageostrophic components associated with this phase of the coastal low coincide with a minimum SLP at San Felix.

Now, ahead of the coastal low, the model predicts that both ageostrophic components are of the same order of magnitude and counteract the effect of the -SLP_{lv} term in the large-scale forcing. Therefore, the SLP_{sf} will tend to remain as the dominant feature in the wind response, as apparent from both composites.

7 Summary and Discussion

The existing offshore LLJ structures in upwelling areas elsewhere, together with limited experimental evidences in our study area, support the theory of a LLJ in the marine layer associated with the average position of the so-called "upwelling front". Maximum theoretical geostrophic speeds at the top of the marine layer, above the front, are compatible with observed SST gradients across it. The observed difference in height of the base of the subsidence inversion base at both sides of the front during an upwelling event, seems also compatible with typical SST values of the coastal and oceanic waters in the area when upwelling is active.

The potential contribution of this LLJ to the surface winds onshore of the upwelling front seems to be related to

a) the daytime coastal lowering of the inversion base enhanced at the leading edge of the coastal low.

b) the progressively colder temperatures close to the coast during an upwelling event, and

c) the role of the ageostrophic wind components in bringing onshore the high-speed, depressed marine layer.

At the same time, an enhancement of the coastal marine layer divergence should result from the opposite zonal components of the ageostrophic winds at both extremes of the upwelling plume, contributing with a positive feedback effect to depress the marine l ayer.

The simple physical model describing the contribution of large to regional horiz ontal pressure gradients and the ageostrophic wind components resulting from time and space changes of that pressure field induced by the propagating coastal lows, seems to properly describe the phase of the alongshore day to day wind variability in the ar ea. In fact, composite analyses ahead of the coastal low for the winter and summer halves of the year, indicate that the strength of the coastal winds is enhanced due to a combination of the large- scale forcing, represented by the pressure rise following a frontal disturbance, and the ageostrophic wind components associated to the leading edge of the coastal low. At the culmination of the low and the following day, both forcing agents bring the winds to a minimum, due to the negative contribution of the ag eostrophic components at that time.

Several aspects, besides the very modest experimental data available in and around the study area, limit the representativeness of the results discussed here. First, not always the base of the inversion coincides with the top of the marine layer (Garratt, 1992), since that requires a fully coupled boundary layer. In fact, more than one cloud layer was apparent in some of the flights during the November 1987 experiment (Fuenzalida et al., 1990). Also, the strong wind shear associated with the LLJ structures is normally a sign of uncoupling below the subsidence inversion.

Another aspect to be considered here, is that the edge of the cloud- topped marine layer should also enhance the tilt of the base of the subsidence invers ion, since the divergence of the infrarred flux producing the cooling is more effective there than in the nearby clear areas.

Finally, the years 1991 and 1992, from which the composite analyses have been performed, corresponded to an El Nino event.

In order to perform a proper model calibration, both the time and space resolution of the coastal and offshore data, have to be improved. An ongoing Project to monitor winds and surface pressure at seven coastal sites from 27 to 33 S in central Chile, with automatic meteorological stations, will soon provide further insight into this modelling problem.

Also, the assessment of the space and time structure of the surface winds over the ocean by means of SSMI and scatterometer satellite data, seems to be promising, as better algorithms and corrections for the coastal area are gradually being introduced.

The mooring of a meteorological buoy at the offshore extreme of the study area is being intended again, after the failure of the first attempt.

The possibility of performing new airborne measurements in the area, incorporating wind and humidity measurements, is also being considered for the near future.

Acknowledgments

The San Felix data were kindly made available by the Meteorological Service of the chilean Navy, while the National Fisheries Service (SERNAP IV) helped substantially in the maintenance of the Point Lengua de Vaca automatic station. The author is indebted to Zaida and Hugo Salinas for the data processing. He would like to thank Professor Abdus Salam, the International Atomic Energy Agency and UNESCO for hospitality at the International Center for Theoretical Physics, Trieste where this work was completed. The study has been possible through the funding of the Project Marine Natural Resources (SAREC- CONICYT) and by the Marine Sciences Development Program of the University o f Chile, under Grant DTI-13667-9313.

REFERENCES

Bakun A. and C. Nelson , 1991, *The seasonal cycle of the windstress curl in subtropical eastern boundary current regions*, J. Phys. Ocean. **21**(12) 1815-1834.

Beardsley R., C. Dorman, A. Friehe, K. Rosenfeld and C. Winnant , 1987, *Local atmospheric forcing during the Coastal Ocean Dynamics Experiment. 1. A description of the marine boundary layer and atmospheric conditions over a northern California upwelling region*, J. Geoph. Res. **92**(C2) 1467-1488.

Bunker A. F. , 1965, *A low-level jet produced by air, sea and land interactions* (cited by Zembra and Friehe, 1987).

Dorman C. E. , 1987, *Possible role of gravity currents in northern California's coastal summer wind reversals*, J. Geoph. Res. **92**(C2) 1497-1506.

Elliot D. and J. O'Brien , 1977, *Observational studies of the marine boudary layer over an upwelling region*, Mo. Wea. Rev. 105 86-98.

Enfield D. , 1981, *Thermally driven wind variability in the planetary boundary layer above Lima, Peru*, J. Geoph. Res., **86**, 2005-2016.

Fuenzalida H. , 1985, *Estructura y comportamiento invernal de la capa limite atmosferica sobre Antofagasta*, Chile. Tralka (2) 4 405-418.

Fuenzalida H., J. Rutllant, J. Vergara , 1990, *Estudio de los estratocumulos costeros y su potencial como recurso hidrico*, Final Report Project 511-88 (FONDECYT-CHILE).

Garratt J. R. , 1992, *The atmospheric boundary layer. Cambridge Atmospheric and Space Science Series.*

Gill A. , 1982, *Atmosphere-Ocean dynamics*, Academic Press.

Haltiner and Martin , 1957, *Physical and Dynamical Meteorology*, Academic Press.

Hsu S. A. , 1988, *Coastal Meteorology*, Academic Press.

Lettau H. , 1967, *Small to large scale features of the boundary layer structure over mountain slopes*, Proc. Symposium on Mountain Meteorology. Fort Collins, Colorado (USA).

Lettau H. and K. Lettau , 1978, *Exploring the world's driest climate*, Report 101, Institute for Envirommental Studies. University of Wisconsin, Madison (USA).

Neiburger M., D. S. Johnson, and C. Chien , 1961, *Studies of the structure of the atmosphere over the eastern Pacific ocean in summer.* Part I *The inversion over the eastern north Pacific ocean*, Univ. Calif. Publ. Meteorol. 1, 1-94

Reason C.J.C., and M.R. Jury , 1990, *On the generation and propagation of the southern Africa coastal-low*, Q. J. R. Meteorol. Soc., **116**, 1133-1151.

Rutllant, J. , 1977, *On the extreme aridity of coastal and Atacama deserts in northern Chile.* Ph.D. Thesis University of Wisconsin, Madison (USA).

Rutllant J., and P. Ulriksen , 1979, *Boundary layer dynamics of the extremely arid northern part of Chile The Antofagasta Field Experiment.* Boundary Layer Meteorol. **17** 41-55.

Rutllant J. , 1990, *Natural desertification mechanisms along the arid west coast of South America*, in *Sand Transport and Desertification in Arid Lands*, (F. El-Baz, I.A. El-Tayeb and M.H.A. Hassan, eds.) World Scientific. 235-252.

Rutllant J., 1993 , *Coastal lows and associated southerly wind events in north-central Chile. Preprints V Int. Conf. on Southern Hemisphere Meteorology and Oceanography.* Hobart, Australia. American Meteorological Society. p. 268-269

Rutllant J. , 1994a, *On the meteorological forcing of the upwelling favorable winds along the chilean coast at 30 S.* Submitted to Contributions in Atmospheric Physics. March 1994.

Rutllant J. , 1994b, *On the generation of coastal lows in central Chile*, Submitted as an Internal Report. International Centre for Theoretical Physics. Trieste, Italy. July 1994.

Rutllant J, V. Montecino, J. Moraga and M. Farias. , 1994 *Coastal air-sea interaction and primary productivity experiments at 29.5 S, 71.5 W*, Submitted for publication in Ciencias Marinas (Mexico).

Uribe E. and S. Neshiva , 1983, *Phytoplankton pigments from the Nimbus VII Coastal Zone Color Scanner Coastal waters off Chile from 18 to 40 S.* Proc. Int. Conf. on Marine Resources of the Pacific. Vina del Mar, Chile. pp 33-40.

Schubert W. H. , 1976, *Experiments with Lilly's cloud-topped mixed layer model*, J. Atmos. Sci. 33 436-446.

Zemba J., and C. A. Friehe , 1987, *The marine atmospheric boundary layer jet in the Coastal Ocean Dynamics Experiment*, J. Geophys. Res. **92**(C2) 1489-1496.

FIGURE CAPTIONS

1. Vertical temperature profiles at the coast (solid lines) and at 50 km offshore Cruz Grande (29.5 S) (dashed lines) performed at 9 hours LT with an airborne Rosemont thermometer and a standard airplane altimeter, for November 6 and 7, 1987.

2. Baroclinic zones within a zonal cross-section of the marine layer from west (left) to east (right) at the subtropical west coast of South America and associated low-level jets (LLJ's) at the upwelling-front and at the coast. Colder (C) and warmer (W) areas are depicted, (Adapted from Rutllant, 1994).

3. Schematic map of three consecutive isallobaric synoptic analyses performed for June 27, 1991 at 12 UT (dotted lines), 18 UTC (dashed lines) and 24 UTC (solid lines. The isallobars are in hPa/6 hours, covering the coastal area of western South America from 20 to 35 S.

4. Composite of eight 5-day wind events centered at day (0), when the pressure reached its minumum value (culmination of the coastal low). Daily values of the surface pseudo-stress of the wind (solid), pressure at 21 UTC at Point Lengua de Vaca (dashed), and pressure at 21 UTC at San Felix island (dotted) are depicted for the winter h alf of the year (a). The pressure difference between San Felix and Point Lengua de Vaca (solid) and the daily-averaged meridional wind speeds at San Felix island (dashed), are included in (b). All the values are departures from the averages listed in Table 1.

5. Same as 4., but for the summer half of the year.

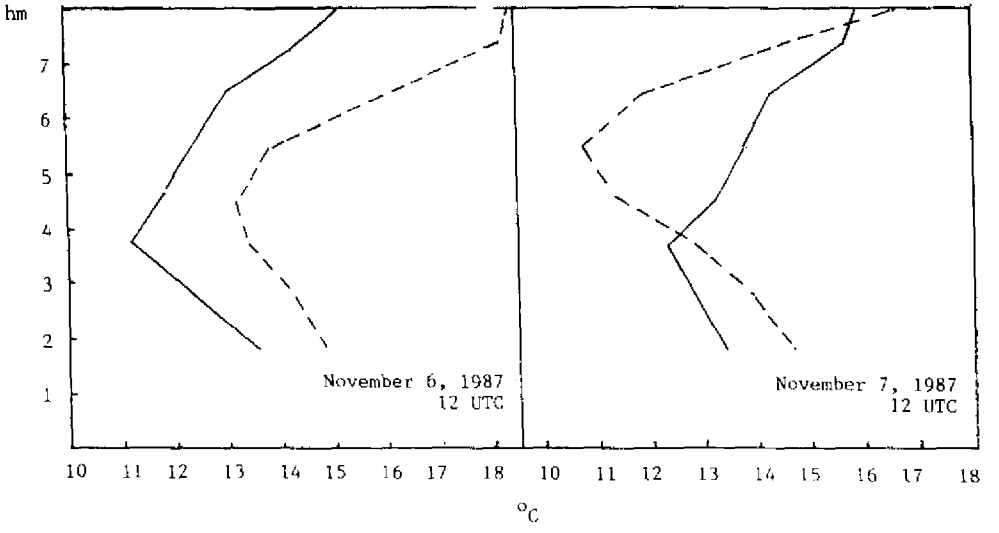

Fig.1

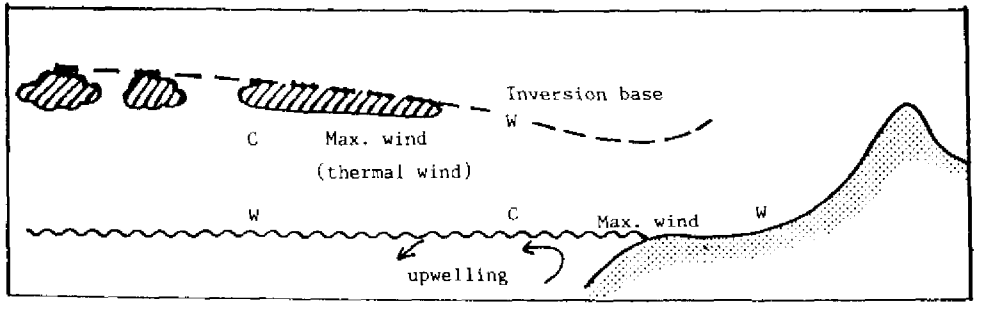

Fig.2

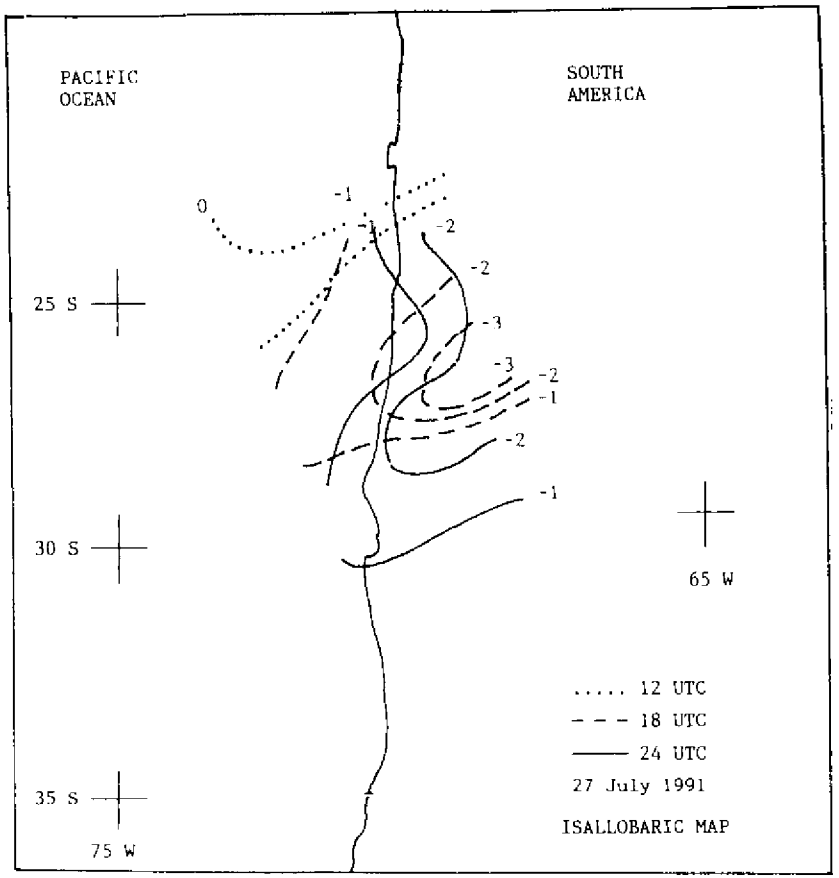

Fig.3

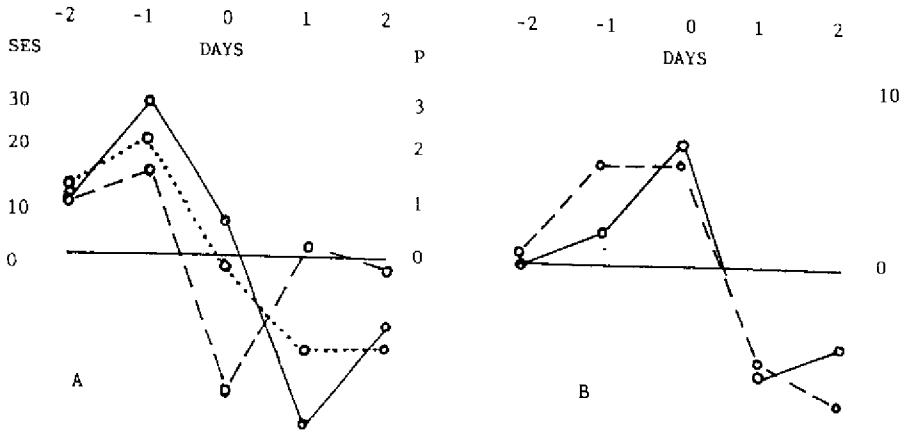

Fig.4

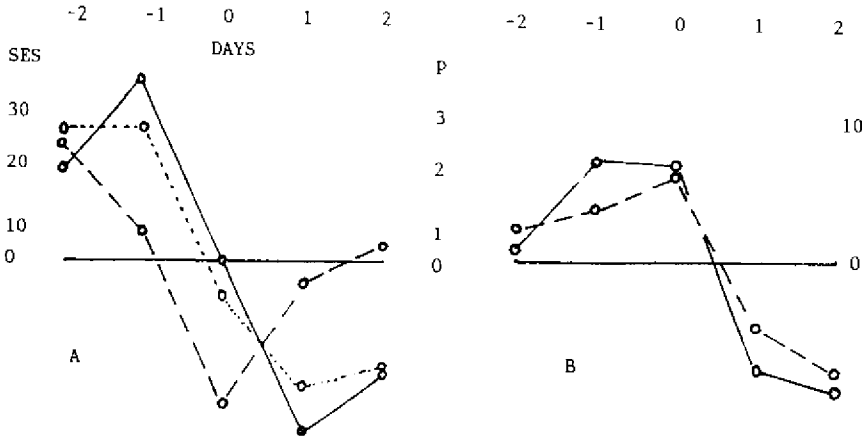

Fig.5